Environmental Fluid Mechanics
https://doi.org/10.1007/s10652-022-09872-3

ORIGINAL ARTICLE

Eddy diffusivity in stratified ocean: a case study in Bay of Bengal

I. D. Lozovatsky[1] · H. J. S. Fernando[1,2] · S. U. P. Jinadasa[3] · H. W. Wijesekera[4]

Received: 16 August 2021 / Accepted: 2 May 2022

Abstract

The eddy diffusivity in the ocean pycnocline $K_N = \gamma\varepsilon/N^2$ is analyzed based on field measurements of the turbulent kinetic energy (TKE) dissipation rate $\varepsilon(z)$ and buoyancy frequency $N(z)$ profiles and an assumed mixing efficiency of $\gamma = 0.2$. The microstructure measurements were taken between 2013 and 2019 in various regions of the Bay of Bengal (BoB) as well as the central Gulf Stream (GS) and deep waters of the Southern California Bight (SCB). The space–time variability of $K_N(z,t)$ observed in the pycnocline of the southeastern BoB is likely related to internal-wave generated turbulence, identified by its following of MacKinnon–Gregg scaling (MacKinnon and Gregg in J Phys Oceanogr 33(7):1476–1492, 2003). The probability distribution function of diffusivity $CDF(K_N)$ could be well fitted by generalized extreme value distribution (GEVD) for all regions of BoB and other oceans. Mixing rates in the upper pycnocline of BoB during extended southwestern monsoon period tend to be larger in the southern parts of the Bay compared to central and northern parts. Statistics of K_N in the GS and SCB waters appear to be similar to those in the southern BoB with a characteristic median value ~ 2×10^{-6} m^2/s, suggesting relatively low intensity of vertical mixing therein compared to the canonical pycnocline diffusivity of $K_N \approx 10^{-5}$ m^2/s.

Article Highlights

- Internal wave instabilities appear to be a dominant mechanism of generating energetic mixing events in the Bay of Bengal (BoB).
- Mixing rates (diffusivities) in the upper pycnocline tends to be larger in the southern BoB than in the northern part of the Bay.

✉ I. D. Lozovatsky
i.lozovatsky@nd.edu

[1] Department of Civil and Environmental Engineering and Earth Sciences, University of Notre Dame, Notre Dame, IN 46556, USA

[2] Department of Aerospace and Mechanical Engineering, University of Notre Dame, Notre Dame, IN 46556, USA

[3] Department of Oceanography, The Ocean University of Sri Lanka, Crow Island, Colombo 15, Sri Lanka

[4] Naval Research Laboratory, Stennis Space Center, 1020 Balch Blvd, Stennis Space Center, MS 39529, USA

- Generalized extreme value distribution approximates well the probability functions of the diffusivity in all tested regions of BoB as well as in the other oceans.

Keywords Ocean mixing · Eddy diffusivity · Dissipation rate · Ocean pycnocline · Bay of Bengal

1 Introduction

Understanding and quantification of turbulent mixing in stably stratified oceans continue to be of great importance in ocean sciences for many decades. In the ocean, vertical (or diapycnal) mixing in stably stratified layers is signified by the buoyancy flux $\overline{b'w'}$, where $b' = -g\frac{\rho'}{\rho_0}$ are the buoyancy fluctuations, ρ_0 the reference density, g the gravity, w' the fluctuations of vertical velocity and overbar denotes appropriate time or space averaging. In numerical models of ocean circulation, turbulent fluxes of momentum and scalars (e.g., buoyancy flux) are usually specified via the mean gradient (e.g., $d\bar{b}/dz$) and a coefficient of exchange K_b known as the eddy diffusivity,

$$\overline{b'w'} = -K_b \frac{\partial \bar{b}}{\partial z}. \tag{1}$$

The eddy diffusivity (or simply diffusivity) is conventionally evaluated based on the assumption of stationarity and horizontal homogeneity of turbulent kinetic energy (TKE) that yields a balance between the TKE production by mean shear P, viscous dissipation ε and work against buoyancy forces $B = -\overline{b'w'}$. Defining the ratio between B and ε as the mixing efficiency,

$$\gamma = B/\varepsilon, \tag{2}$$

and combining (1) and (2), the diffusivity $K_b \equiv K_N$ becomes,

$$K_N = \gamma \frac{\varepsilon}{N^2}. \tag{3}$$

where $N^2(z) = g/\rho_0 \frac{\partial \rho}{\partial z}$ is the squared buoyancy frequency, z is positive downward, and $z=0$ at the sea surface. The use of subscript N signifies approximations used in deriving (3) from (1). Osborn [2] suggested that $\gamma \approx 0.2$, but later it has been argued that γ could be a function of the Richardson and buoyancy Reynolds numbers (e.g., Lozovatsky and Fernando [3]; also see more recent findings of Gregg et al. [4], Garanaik and Venayagamoorthy [5], and Conry et al. [6]). The success of oceanic in-situ measurements of $\varepsilon(z)$ over last several decades (e.g., [7–11]) permitted estimating eddy diffusivity and therefore mixing rates in various regions of the World Ocean. Another method of estimating oceanic diffusivity is the use of microscale temperature measurements to calculate the dissipation rate χ of turbulent temperature fluctuations and using a diffusivity in the form $K_T = \frac{\chi}{2\left(d\bar{T}/dz\right)^2}$ (e.g., [12, 13]). An indirect method based on internal-wave strain estimates and corresponding fine-scale parameterizations is also used (e.g., [7, 14, 15]). In this study, we focus on the most direct and reliable estimates of diffusivity in the upper pycnocline of the Bay of Bengal (BoB) based on Eq. (3) with a canonical mixing efficiency $\gamma = 0.2$ [4, 8].

Recent publications on mixing rates in BoB [16] revealed a strong functional dependence of K_N on the gradient Richardson number $Ri = N^2/Sh^2$

$$K_N = \frac{K_o}{\left(1 + Ri/Ri_{cr}\right)^s} + K_{br}, \tag{4}$$

where Sh is the vertical shear. For the background diffusivity $K_{br} = 10^{-6}$ m^{2}s^{-1}, critical Richardson number $Ri_{cr} = 0.25$ and for $Ri << Ri_{cr}$, the mixing exchange coefficient K_o is close to 10^{-4} m^{2}s^{-1}. It is possible that the power of Ri in (4) has a universal value $s = 2$, as it provides the best fit to the published BoB data as well as data collected recently near the Nova Scotia shelf break [17] and data from nocturnal atmospheric stably stratified layers [3].

A seasonal cycle of mixing along 8°N of BoB has been reported by Cherian et al. [13] with strongest turbulence observed between July and November, corresponding to the extended southwestern monsoon season. Enhanced diffusivities were observed by Luecke et al. [18] during the passage of a sub-surface anti-cyclonic eddy in the western BoB. The seasonality of the upper-ocean turbulence in the central (12°N) and northern (18°N) BoB has been discussed by Warner et al. [19], and the suppression of turbulence during the latter part of the southwestern monsoon due to enhanced stratification resulting from the freshwater input has been observed by Thakur et al. [20]. While acknowledging these important findings, this paper addresses the question: how variable are the mixing rates in the upper pycnocline of BoB during relatively short time periods (~ week) in various locations separated by ~ 100 miles and more. A statistical analysis (probability distribution functions) is conducted on estimated diffusivities, and compared with corresponding turbulence data obtained in and around BoB as well as in several other deep-ocean regions of the world.

2 Data

The most recent turbulence measurements in the BoB were carried out in June 2019 onboard of the R/V Sally Ride as a part of the MISO-BoB research initiative. Measurements taken by a VMP-500 microstructure profiler (e.g., Wolk et al. [21] in the southeastern part of the Bay ($\varphi = 8°$N, $\lambda = 89°$E) as well as along a meridional transect ($\lambda = 86°$E) at the latitudes $\varphi = 8°$N, 10°N, 12°N, and 14°N are the focus of this paper. In particular, we analyze the estimates of eddy diffusivity (Eq. 3) in the upper ocean pycnocline below surface mixed layer. The TKE dissipation rate $\varepsilon(z)$ and the buoyancy frequency $N(z)$ were obtained in a series of consecutive VMP casts (from 4 up to 25 profiles at each location) with vertical resolution $\Delta z \sim 1.4$ m (2 s averaging for VMP sinking velocity ~ 0.7 m/s). The upper pycnocline depth varied at different locations between $z > 40$–65 and $z < 170$–210 m. The methodology of the VMP data processing was the same as in [16], which followed Roget et al. [22] framework.

These 2019 BoB diffusivity estimates were subjected to a comprehensive statistical analysis and compared with K_N from our previous turbulence measurements in the region. In 2013, the dissipation measurements were taken in the northern BoB [23]. In 2014, the data were collected along two sections to the south and to the east of Sri Lanka [11, 23]. In 2018, a field campaign was carried out in the western BoB [16] during the presence of a cyclonic mesoscale eddy, commonly known as the Sri Lanka Dome. We also explored two regions of deep ocean in different localities, namely a central section of the Gulf Stream [24] and Southern

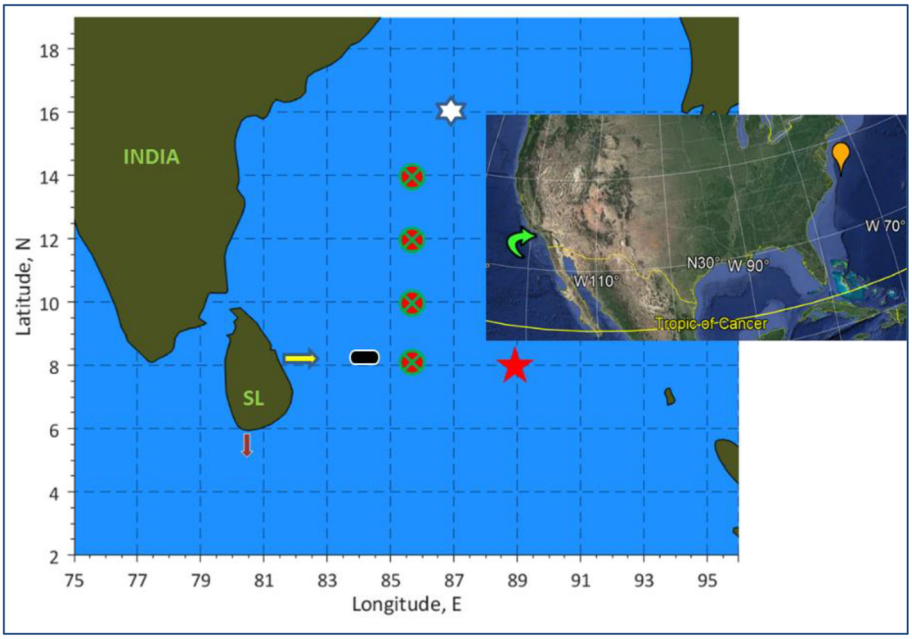

Fig. 1 Locations of the VMP measurements taken in the Bay of Bengal in 2013–2014 and 2018–2019 (abbreviations are in Table 1): 1—white hexagon (2013, 16Nc); 2—brown arrow (2014, WS also SMC); 3—light-yellow arrow (2014, TS also 8Neicc); 4—dark-blue oval (2018, 8Nsld and 8Nw); 5—red-green crossed circles (2019, 8Nc, 10Nc, 12Nc, 14Nc); 6—red pentagram (2019, 8Ne). In the insert: VMP measurements in the Atlantic—orange bulb (2015, GSs) and in the Pacific—green curved arrow (2017, SCB)

California Bight [25]. Figure 1 shows schematic locations of the analyzed data, and Table 1 gives details of measurements.

3 2019 Data analysis of the BoB pycnocline diffusivities

3.1 Internal-wave induced turbulence and mixing

A 3-h long time series of 25 diffusivity profiles obtained in the southeastern BoB ($\varphi = 8°$N, $\lambda = 89°$E, red star in Fig. 1) is shown in Fig. 2 to illustrate the short-term variability of mixing in the pycnocline below the surface mixed layer (the depth range 50–60 m $< z <$ 150–180 m). An interesting pattern of 'layering' that consists of alternating (blue and yellow) bands of diffusivity $K_N(z, t)$, which is outlined in Fig. 2 in a background of wave-like variations of isothermal surfaces in the pycnocline, could point to internal-wave induced turbulence and mixing (e.g., [14, 26, 27]). If this conjecture is valid, then the TKE dissipation rate $\varepsilon(z)$, which mainly affects $K_N(z)$ in an approximately linearly stratified pycnocline could be parametrized as [1].

$$\varepsilon = \varepsilon_{MG} \equiv \varepsilon_0 \frac{N}{N_0} \frac{Sh}{Sh_0}, \tag{5}$$

Where N and Sh are suitably averaged values of buoyancy frequency and vertical shear, respectively, N_0, Sh_0 (= 3 cph), and ε_0 are background values for a specific time period.

Table 1 The VMP measurement sites 2013–2019

Region, station names and abbreviations, date	Latitude (φ) and longitude (λ)	Ocean depth and pycnocline range Δz	Duration, number of casts
Indian Ocean			
Bay of Bengal (R/V *Roger Revelle*, R/V *Thompson G Thompson* and R/V *Sally Ride* USA) Weligama (WS) and Trincomalee (TS) sections (R/V *Samuddrika*, Sri Lanka)			
Southeastern BoB (8Ne also BoB-19, 8 N 89E): 2019, June 11	φ = 8°N, λ = 89°E	3600 m Δz = 60–170 m	3 h, 24 VMP casts
Central BoB section (BoB-19 and 8Nc, 10Nc, 12Nc, 14Nc): 2019, May 31–June 3	φ = 8°N–14°N, λ = 85.75°E (φ:8°N, 10°N, 12°N, 14°N)	3740–3060 mfrom S to N Δz = 60–170 m Δz = 65–210 m Δz = 45–190 m Δz = 40–165 m	75 h, 16 VMP casts at 4 stations
Western BoB (8Nw): 2018, July 15–16	φ = 8.1°N, λ = 83.7–83.0°E	3780–3800 m Δz = 40–170 m	11 h, 10 VMP castsat 10 stations
Western BoB (8Nsld also SLD-18): 2018, July 16–17	φ = 8.1°N, λ = 84.5–83.7°E	3770–3810 m Δz = 40–165 m	10 h, 10 VMP castsat 10 stations
East Indian Costal Current (8Neicc also TS): 2014, Sep 9–10	φ = 8.0–8.1°N, λ = 81.8–82.6°E	960–3870 m Δz = 60–180 m	17 h, 7 VMP castsat 7 stations
South Monsoon Current (SMC also WS): 2014, April 23–24	φ = 5.92–5.37°N, λ = 80.4°E	1100–4200 m Δz = 40–160 m	16 h, 14 VMP castsat 7 stations
Northern BoB (16Nc also BoB-13): 2013, Nov 18	φ = 15.94–15.96°N, λ = 86.94.3–86.96°E	2740 m Δz = 20–125 m	1.5 h, 12 VMP casts
Pacific Ocean South California Bight (R/V *Sally Ride*, USA)			
SCB, (F4): 2017, Oct 4	φ = 33.76°N, λ = 119°W	900 m Δz = 30–175 m	23 h, 14 VMP casts
Atlantic Ocean Gulf Stream (R/V *Atlantic Explorer*, USA)			
GSs: 2015, Oct 30	φ = 35.83°N, λ = 74.1°W	2660 m Δz = 60–170 m	2 h, 4 VMP casts

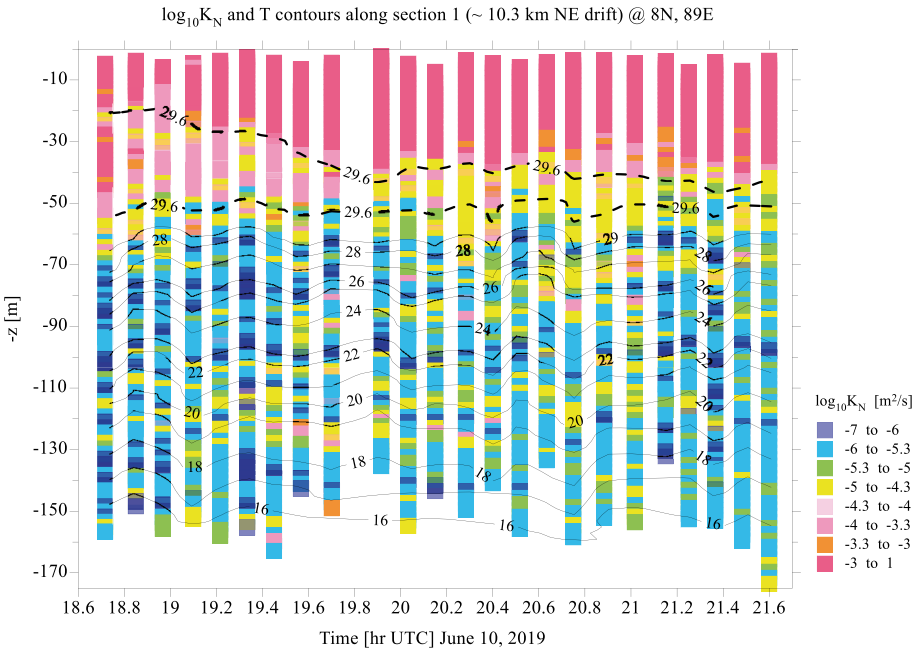

Fig. 2 A 3 h time series of the diffusivity profiles $\log_{10} K_N(z,t)$ (color bars) overlaid by temperature $T(z,t)$ contours. The southeastern BoB (8°N, 89°E), June 11, 2019

It appears from Fig. 3 that for BoB-19 8Ne data (see station abbreviations in Table 1 and in Fig. 1) the MacKinnon–Gregg [1] parameterization holds well for $\varepsilon > (3-4)\times 10^{-9}$ W/kg with an empirical constant $\varepsilon_0 = 4.04\times 10^{-10}$ W/kg and the 95% confidence bounds $\varepsilon_0 = (3.44-4.64)\times 10^{-10}$ W/kg (https://www.mathworks.com/products/curvefitting.html). This relatively high ε_0 indicates significant influence of internal-wave induced turbulence on vertical mixing in this region of the southeastern BoB. Note that MacKinnon and Gregg [1] found $\varepsilon_0 = 6.9\times 10^{-10}$ W/kg for the dynamically active New England shelf, while Sun et al. [28] reported $\varepsilon_0 = 8.6\times 10^{-10}$ W/kg for sufficiently strong turbulence in the northern South China Sea. It is noted that in June 2019, stratification in the southeastern BoB at 8°N, 89°E (8Ne station) did not exhibit a sharp density jump below the surface mixed layer (SML), which is a common observation in the northern BoB (e.g., [23]). As such, the relatively uniform pycnocline was not decoupled from the SML (~50 m deep), allowing an energy flux from SML to penetrate downwards more easily, thus enhancing background mixing in stratified water interior. Note that Vinayachandran et al. [29] and Jenson et al. [30], based on observations in July 2016, reported a periodic development and erosion of a barrier layer between the SML and pycnocline at 8°N, 89°E caused by advection of a shallower, low-saline mixed layer over a deeper isothermal layer. During erosion stage of the barrier layer, the SML deepened up to ~60 m, similarly to what we have observed at the same location in 2019 (Fig. 2).

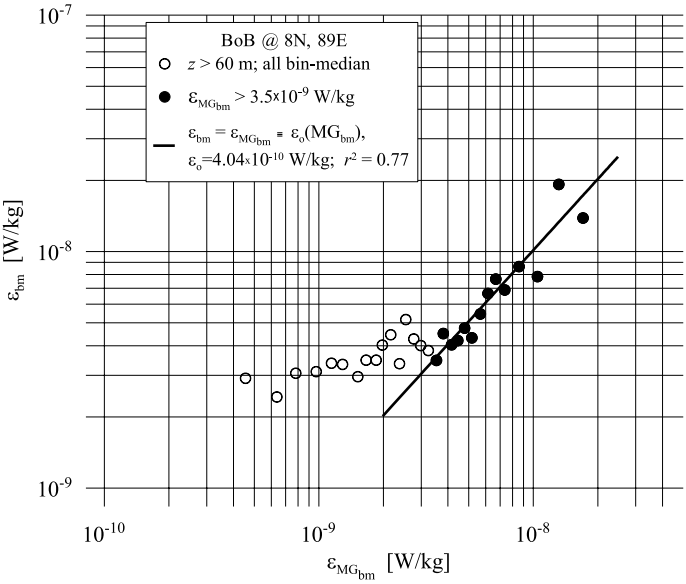

Fig. 3 Bin-median estimates (40 samples per bin) of the TKE dissipation rate ε_{bm} versus the MacKinnon–Gregg [1] parameterization $\varepsilon_{MG_{bm}} \equiv \varepsilon_0\left(\frac{N}{N_0}\frac{Sh}{Sh_0}\right)$, where $N_0 = Sh_0 = 3$ cph and ε_0 is an empirical constant (see text for details)

3.2 Diffusivity statistics of the 2019 BoB data

The cumulative probability distribution functions of diffusivity $CDF\left(K_N\right)\sqrt{b^2-4ac}$ computed for pycnocline measurement at five locations during the 2019 BoB measurements are shown in Fig. 4. All empirical distributions are well approximated by generalized extreme value (GEV) distribution [31, 32].

$$CDF(\tilde{x}) = \exp\left\{-[1+k\tilde{x}]^{-1/k}\right\}, \quad \text{where } \tilde{x} = \left(K_N - \mu\right)/\sigma \tag{6}$$

and the values of shape k, scale σ, and location μ parameters are given in the figure legend. The GEV distribution showed the best maximum likelihood estimate of the fit amongst all probability distribution models offered by Matlab distribution fitter application dfittool (https://www.mathworks.com/help/stats/dfittool.html).

It is clear that four out of five CDFs in Fig. 4 have similar shape factors ($k = 0.87$–1.03) and the scale of distributions gradually decreases from $\sigma = 2 \times 10^{-6}$ to $\sigma = 1 \times 10^{-6}$ W/kg between 8 and 14°N. The $CDF\left(K_N\right)$ at 12°N somewhat deviates from the others curves, with lack of relatively large K_N samples; about 25% of the distribution consists of $K_N > 3 \times 10^{-6}$ m^2/s and only 1% has $K_N > 10^{-5}$ m^2/s. It seems that internal-wave activity at 12°N was relatively low and a "regular number" of intermittent mixing events typical for the pycnocline in the central BoB was not generated at the time of VMP measurements. Nevertheless, the majority (~75%) of K_N samples at 12°N do not diverge from all other CDFs presented in Fig. 4.

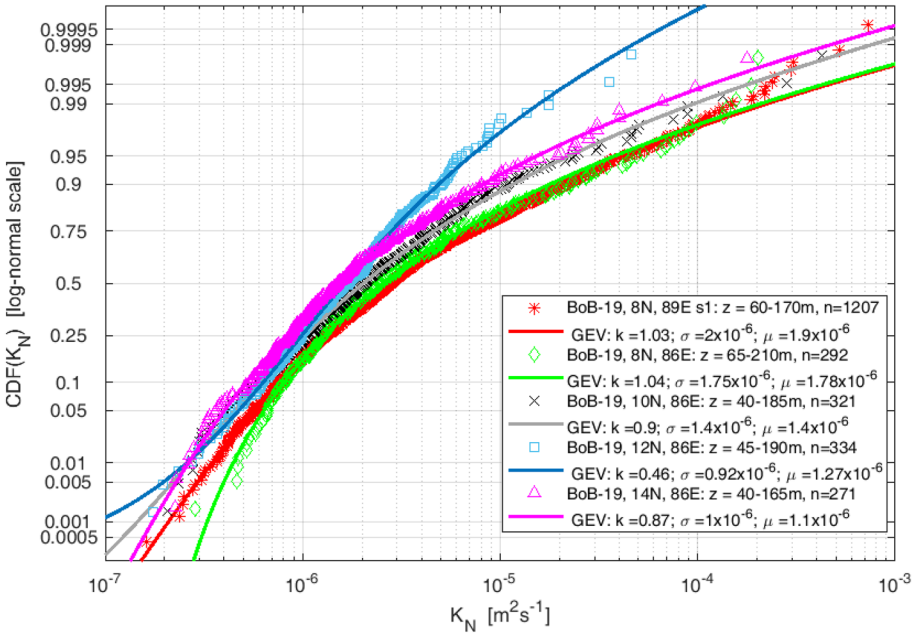

Fig. 4 Cumulative distribution functions of eddy diffusivity $CDF(K_N)$ in the upper pycnocline of BoB calculated based on 2019 VMP measurement taken at 8°N, 89°E and along 86°E meridional section at 8°N, 10°N, 12°N, and 14°N. The depth ranges (z) and a number of samples (n) used for evaluation of $CDF(K_N)$ are in the legend. All observed probability functions are well approximated by generalized extreme value (GEV) distribution with the shape k, scale σ and location μ parameters given in the legend

4 Variability of the pycnocline mixing in BoB and other oceans

More insights on the spatial variability of mixing (diffusivity) in the BoB pycnocline can be drawn from Fig. 5, where $CDF\left(K_N\right)$ at the most southeastern BoB-19 8Ne station is presented together with $CDFs\left(K_N\right)$ obtained in several other BoB regions shown Fig. 1. Two additional distribution functions of K_N are also shown in Fig. 5 to represent mixing rates in other oceanic locations (central Gulf Stream, GSs, and Southern California Bight, SCB) using our VMP measurements taken in 2015 [24] and 2017 [25], respectively. All analyzed $CDF\left(K_N\right)$ are best-fitted by GEV distribution model, being specified and distinguished by the GEV distribution parameters k, σ, μ, that are shown in Fig. 6 along with such important statistical measures as the median values of the diffusivity $med\left(K_N\right)$ and standard deviation $std\left(K_N\right)$.

The $CDF\left(K_N\right)$ in Fig. 5 can be roughly divided into three groups. The first group contains the CDF that belongs to the most northern BoB-13 location 16Nc (magenta triangles), where only ~ 1% of the diffusivities of all 762 analyzed samples exceeded 10^{-5} m^2/s, the largest being $K_N = 5.3 \times 10^{-5}$ m^2/s. The lowest *median* and *std* values of K_N as well as the smallest scale σ and location μ parameters of GEVD (also see Fig. 6) quantify the weakest pycnocline mixing in the northern BoB compared to all other analyzed regions of the Bay.

The second group contains CDFs in the South Monsoon (SMC or WS-14) and East Indian Coastal (8Neicc or TS-14) currents (black pluses and green circles, respectively).

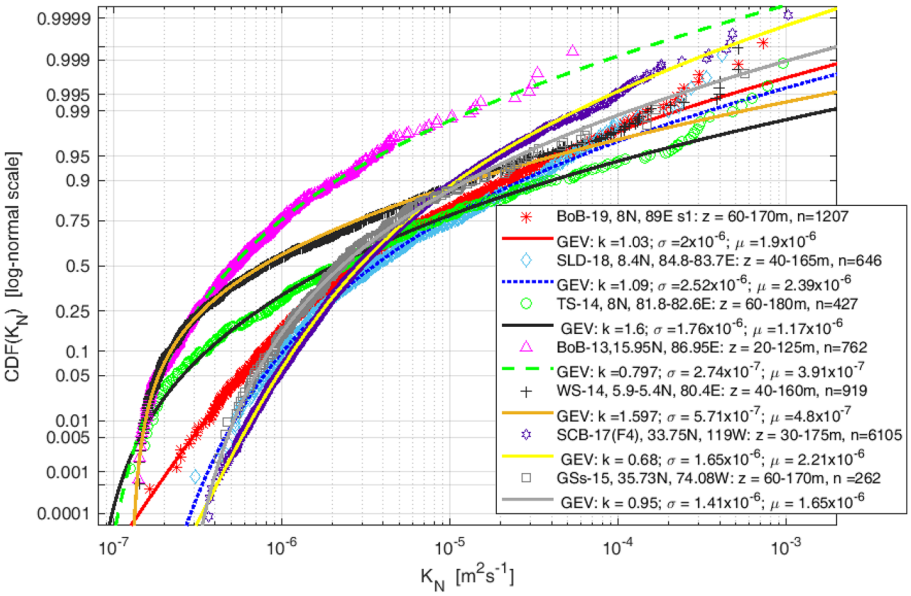

Fig. 5 Cumulative distributions functions of the diffusivity $CDF(K_N)$ in the upper pycnocline based on VMP dissipation and stratification measurements at several representative regions of the BoB in 2013–2014 and 2018–2019 (see Fig. 1 and Table 1 for abbreviations). The BoB probability distributions of K_N are shown along with the pycnocline $CDFs(K_N)$ obtained in deep waters of the South California Bight (SCB-17) and the Gulf Stream (GSs-15). The depth ranges and a number of samples (n) used for $CDF(K_N)$ evaluation are in the legend. All observed probability functions are well approximated by generalized extsssreme value (GEV) distribution with the shape k, scale σ and location μ parameters given in the legend

These CDFs exhibit the largest variability of K_N signified by two largest values of the GEVD shape parameter $k \sim 1.6$ and the largest $std(K_N)$ that are given in Fig. 6. Relatively rare but powerful mixing events in EICC ($K_N > 10^{-4}$ m^2/s) constitute about 5% of the TS-14 distribution. At the same time, relatively high probability of weak turbulence events (defined by left tails of K_N distributions in Fig. 5) could be driven by a variety of shear-induced instabilities in the monsoon influenced boundary currents around Sri Lanka. This contrasts with internal-wave induced instabilities that produce a narrower range of K_N, which arguably prevail in other regions of BoB away from boundary currents.

The third and the densest group of distribution functions in Fig. 5 has a similar shape (see also CDFs in Fig. 4) with the GEVD shape parameter that varies in a narrow range $k = 0.9$–1.1. This may indicate similar (IW-induced) mechanisms of diapycnal mixing in the most of southern and central BoB as well as in the other regions of the open ocean.

Figure 6 summarizes mixing activity in the Bay, comparing it with diffusivities observed in GSs and SCB. It is interesting that a simple but the most representative statistics of the pycnocline mixing rate, $med(K_N)$, gradually decreases from the most southeastern station 8Ne toward the north (14Nc) and then sharply goes down at 16Nc, pointing to the stronger stable stratification resulting from riverine inflow and excess rainfall (e.g., [33, 34]) in the region. The scale and position parameters of GEVD appropriately follow the median estimates for all locations, confirming the usefulness of GEVD as a statistical model for the diffusivity in the ocean pycnocline. In all western measurement regions of BoB, located along 8°N (8Neicc, 8Nw, and 8Nsld), the $med(K_N)$ returns to its characteristic value $\sim 2 \times 10^{-6}$ m^2/s found at 8Nc

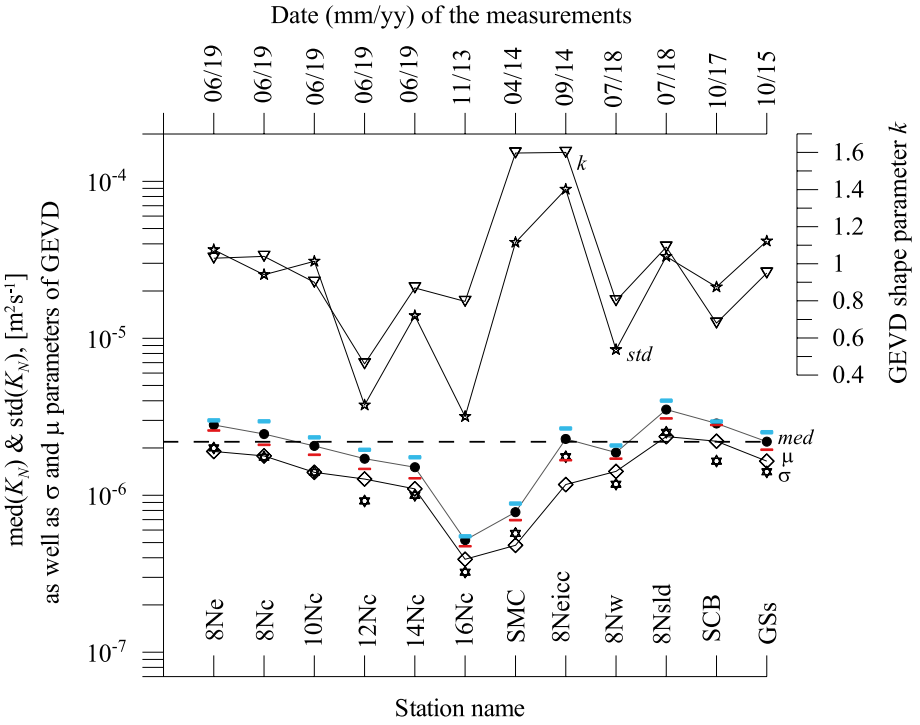

Fig. 6 The shape, k (triangles), scale, σ (hexagrams), and location, μ (diamonds), parameters of generalized extreme value distribution (GEVD) used to approximate empirical distribution functions of K_N at various measurement sites (see Table 1 for name abbreviations). The medians (black circles) flanked by the 95% lower (red) and upper (blue) confidence limits as well as standard deviations (pentagrams) of pycnocline diffusivities are also plotted; the dashed line is the mean value of the medians $\langle med(K_N)\rangle = 2.04 \times 10^{-6}$ m^2/s

and 8Ne in the central and southeastern BoB. Note that a local enhancement of $med\left(K_N\right)$ at 8Nsld, which was occupied in 2018 by a cyclonic eddy (the Sri Lanka Dome) signifies possible enhancement of pycnocline mixing due to mesoscale ocean dynamics [16, 18]. Statistics of the diffusivity in the upper pycnocline of California (SCB) and Gulf Stream (GSs) waters are similar to those found in the southern BoB, indicating relatively low intensity of vertical mixing in those regions comparing to the long-known canonical diffusivity $K_N = 10^{-5}$ m^2/s (e.g., [35, 36]). On the other hand, if the pycnocline diffusivity is characterized by the mean value $mean\left(K_N\right)$, which is a less representative statistic than the median $med\left(K_N\right)$ for heavy-tailed distributions like GEVD, then the $mean\left(K_N\right)$ ranges between 1.8×10^{-6} and 2.5×10^{-5} m^2/s for all our measurement locations, with the averaged mean of the means $\left\langle mean\left(K_N\right)\right\rangle = 9 \times 10^{-6}$ m^2/s, which is close to the canonical pycnocline diffusivity 10^{-5} m^2/s.

5 Summary

A robust statistical analysis of eddy diffusivity $K_N = 0.2\varepsilon/N^2$ in the upper-ocean pycnocline evaluated using in situ measurements of the TKE dissipation rate $\varepsilon(z)$ and buoyancy gradient $N^2(z)$ taken during multiple field campaigns in the Bay of Bengal (BoB) or its proximity was presented in this paper, with the most recent measurements conducted in June 2019 onboard the R/V Sally Ride. The turbulence data were collected using a VMP-500 microstructure profiler in the southeastern BoB ($\varphi = 8°$N, $\lambda = 89°$E) as well as along a meridional, $\lambda = 86°$E, transect at the latitudes $\varphi = 8°$N, 10°N, 12°N, and 14°N. The diffusivities (mixing rates) of the 2019 field campaign were compared with K_N estimates from our previous measurements (i) in the northern BoB [23]; (ii) at two sections to the south and to the east from Sri Lankan coast [10, 23]; (iii) across the Sri Lanka Dome in the southwestern BoB [16], and (iv) in two distant deep-ocean regions away from the BoB, namely central Gulf Stream [24] and Southern California Bight [25]. A hypothesis on the dominant influence of internal-wave instability on turbulence generation in the pycnocline of southeastern BoB was explored based on the notion that kindred turbulence obeys the MacKinnon–Gregg [1] dissipation parameterization. The observed vertical 'layered structure' of diffusivity therein appears to be consistent with the above hypothesis.

All cumulative probability distribution functions for the pycnocline $CDF(K_N)$ were well fitted by a three-parameter generalized extreme value distribution (GEVD), the most flexible probability model that describes extreme events [37], suggesting highly intermittent (in space and time) nature of pycnocline mixing in all studied regions of BoB and elsewhere alluded to in this paper. Therefore, from the probabilistic point of view vertical mixing in the upper part of the main oceanic pycnocline, defined here by K_N, can be considered as a sequence of extreme random events. This requires non-stationary sources of turbulent energy such as intermittent internal-wave breaking and sporadic shear-induced instabilities.

It was found that representative statistics of the pycnocline mixing such as the median of diffusivities $med(K_N)$ gradually decreases from the most southeastern BoB stations at 8°N toward the north stations (14°N). It then sharply goes down at 16°N, being affected by strong stratification caused by the riverine input and excessive monsoon rainfall in the northern BoB [33]. In all western measurement stations of the Bay located along 8°N, $med(K_N)$ returns to its characteristic value $\sim 2 \times 10^{-6}$ m^2/s found in the central and eastern BoB during summer monsoon period. Some elevation of $med(K_N)$ associated with a cyclonic eddy–the Sri Lanka Dome was noted, indicating possible enhancement of mixing by mesoscale ocean dynamics [16, 18], which, in turn, is linked to seasonal forcing (e.g., [19, 20, 34]). Statistics of the diffusivity in the upper pycnocline of California (SCB) waters and central Gulf Stream (GSs) are similar to those in the southern BoB. This indicates relatively low intensity of vertical mixing in those regions as compared to the long-held value of canonical diffusivity $K_N = 10^{-5}$ m^2/s (e.g., [4, 35, 36]) based on measurements in various regions of the World Ocean.

Acknowledgements Support for ship operation was provided by the US Office of Naval Research (ONR) and Naval Research Laboratory. We acknowledge funding the participants of University of Notre Dame through ONR Grant N00014-17-1-2334.

Data availability The dataset analyzed in the current study can be made available to the interested researchers by contacting Iossif Lozovatsky (ilozovat@nd.edu).

References

1. MacKinnon JA, Gregg MC (2003) Mixing on the late-summer New England shelf—solibores, shear, and stratification. J Phys Oceanogr 33(7):1476–1492
2. Osborn TR (1980) Estimates of the local rate of vertical diffusion from dissipation measurements. J Phys Oceanogr 10:83–89. https://doi.org/10.1175/1520-0485(1980)010%3c0083:EOTLRO%3e2.0.CO;2
3. Lozovatsky I, Fernando HJS (2013) Mixing efficiency in natural flows. Philos Trans R Soc A 371:20120213. https://doi.org/10.1098/rsta.2012.0213
4. Gregg MC, D'Asaro EA, Riley JJ, Kunze E (2018) Mixing efficiency in the ocean. Annu Rev Mar Sci 10:443–473. https://doi.org/10.1146/annurev-marine-121916-063643
5. Garanaik A, Venayagamoorthy SK (2019) On the inference of the state of turbulence and mixing efficiency in stably stratified flows. J Fluid Mech 867:323–333
6. Conry P, Kit E, Fernando HJS (2020) Measurements of mixing parameters in atmospheric stably stratified parallel shear flow. Environ Fluid Mech 20:1177–1197. https://doi.org/10.1007/s10652-018-9639-z
7. Gregg M (1989) Scaling turbulent dissipation in the thermocline. J Geophys Res 94:9686–9698
8. Oakey N (1982) Determination of the rate of dissipation of turbulent energy from simultaneous temperature and velocity shear microstructure measurements. J Phys Oceanogr 12:256–271
9. Moum JN, Gregg MC, Lien RC, Carr ME (1995) Comparison of turbulence kinetic energy dissipation rate estimates from two ocean microstructure profilers. J Atmos Ocean Technol 12:346–366
10. Lozovatsky I, Roget E, Fernando HJS, Figueroa M, Shapovalov S (2006) Sheared turbulence in a weakly-stratified upper ocean. Deep Sea Res I 53:387–407
11. Lozovatsky I, Fernando HJS, Planella-Morato J, Zhiyu L, Lee JH, Jinadasa SUP (2017) Probability distribution of turbulent kinetic energy dissipation rate in ocean: observations and approximations. J Geophys Res Oceans 122:8293–8308
12. Osborn TR, Cox CS (1972) Oceanic fine structure. Geophys Fluid Dyn 3:321–345
13. Cherian DA, Shroyer EL, Wijesekera HW, Moum JN (2020) The seasonal cycle of upper-ocean mixing at 8°N in the Bay of Bengal. J Phys Oceanogr 50:323–342. https://doi.org/10.1175/JPO-D-19-0114.1
14. Polzin KL, Toole JM, Schmitt RW (1995) Finescale parameterizations of turbulent dissipation. J Phys Oceanogr 25:306–328
15. Kunze E (2017) Internal-wave-driven mixing: global geography and budgets. J Phys Oceanogr 47:1325–1345. https://doi.org/10.1175/JPO-D-16-0141.1
16. Lozovatsky I, Pirro A, Jarosz E, Wijesekera HW, Jinadasa SUP, Fernando HJS (2019) Turbulence at the periphery of Sri Lanka dome. Deep Sea Res II 168:104614. https://doi.org/10.1016/j.dsr2.2019.07.002
17. Lozovatsky I, Wainwright C, Creegan E, Fernando HJS (2020) Ocean turbulence and mixing near the shelf break south-east of Nova Scotia. Bound-Layer Meteorol. https://doi.org/10.1007/s10546-020-00576-z
18. Luecke CA, Wijesekera HW, Jarosz E, Wang DW, Wesson JC, Jinadasa SUP, Fernando HJS, Teague WJ (2021) Observations of eddy-modulated turbulent mixing in the southern Bay of Bengal. J Phys Oceanogr 51:2149–2166. https://doi.org/10.1175/JPO-D-20-0280.1
19. Warner SJ, Becherer J, Pujiana K, Shroyer EL, Ravichandran M, Thangaprakash VP, Moum JN (2016) Monsoon mixing cycles in the Bay of Bengal: a year-long subsurface mixing record. Oceanography 29(2):158–169. https://doi.org/10.5670/oceanog.2016.48
20. Thakur R, Shroyer EL, Govindarajan R, Farrar JT, Weller RA, Moum JN (2019) Seasonality and buoyancy suppression of turbulence in the Bay of Bengal. Geophys Res Lett 46:4346–4355. https://doi.org/10.1029/2018GL081577
21. Wolk F, Yamazaki H, Seuront L, Lueck RG (2002) A new free-fall profiler for measuring biophysical microstructure. J Atmos Ocean Technol 19:780–793. https://doi.org/10.1007/s10872-018-0474-0
22. Roget E, Lozovatsky I, Sanchez X, Figueroa M (2006) Microstructure measurements in natural waters: methodology and applications. Prog Oceanogr 70:123–148
23. Jinadasa SUP, Lozovatsky I, Planella-Morató J, Nash JD, MacKinnon JA, Lucas AJ, Wijesekera HW, Fernando HJS (2016) Ocean turbulence and mixing around Sri Lanka and in adjacent waters of the northern Bay of Bengal. Oceanography 29:170–179. https://doi.org/10.5670/oceanog.2016.49
24. Lozovatsky I, Planella-Morato J, Shearman K, Wang Q, Fernando HJS (2017) Eddy diffusivity and elements of mesoscale dynamics over North Carolina shelf and contiguous Gulf Stream waters. Ocean Dyn 67:783–798. https://doi.org/10.1007/s10236-017-1059-y

25. Lozovatsky I, Shearman K, Pirro A, Fernando HJS (2019) Probability distribution of turbulent kinetic energy dissipation rate in stratified turbulence: microstructure measurements in the Southern California Bight. J Geophys Res Oceans 124:4591–4604. https://doi.org/10.1029/2019JC015087
26. Lozovatsky I, Wijesekera H, Jarosz E, Lilover M-J, Pirro A, Silver Z, Centurioni L, Fernando HJS (2016) A snapshot of internal waves and hydrodynamic instabilities in the southern Bay of Bengal. J Geophys Res Oceans 121:5898–5915. https://doi.org/10.1002/2016JC011697
27. Lozovatsky I, Lee J-H, Fernando HJS, Kang SK, Jinadasa SUP (2015) Turbulence in the East China Sea: the summertime stratification. J Geophys Res Oceans 120:1856–1871. https://doi.org/10.1002/2014JC010596
28. Sun H, Yang Q, Tian J (2018) Microstructure measurements and finescale parameterization assessment of turbulent mixing in the northern South China Sea. J Oceanogr 74:485–498
29. Vinayachandran PN et al (2018) BoBBLE ocean–atmosphere interaction and its impact on the South Asian Monsoon. Bull Am Meteorol Soc 99:1569–1587. https://doi.org/10.1175/BAMS-D-16-0230.1
30. Jenson VG, Vinayachandran PN, Vijith V, Thushara V, Nayak AA, Pargaonkar SM, Amol P, Vijaykumar K, Matthews AJ (2019) Mechanisms of barrier layer formation and erosion from in situ observations in the Bay of Bengal. J Phys Oceanogr 49:1183–1200. https://doi.org/10.1175/JPO-D-18-0204.1
31. Jenkinson AF (1955) The frequency distribution of the annual maximum (or minimum) values of meteorological elements. Q J R Meteorol Soc 81(348):158–171. https://doi.org/10.1002/qj.49708134804
32. Bali TG (2003) The generalized extreme value distribution. Econ Lett 79:423–427
33. Sengupta D, Bharath Raj GN, Ravichandran M, Sree Lekha J, Papa F (2016) Near-surface salinity and stratification in the north Bay of Bengal from moored observations. Geophys Res Let 43:4448–4456
34. Sree Lekha J, Buckley JM, Tandon A, Sengupta D (2018) Subseasonal dispersal of freshwater in the northern Bay of Bengal in the 2013 summer monsoon season. J Geophys Res Oceans 123:6330–6348. https://doi.org/10.1029/2018JC014181
35. Ledwell JR, Watson AJ, Law CS (1993) Evidence for slow mixing across the pycnocline from an open-ocean tracer-release experiment. Nature 364:701–703
36. Toole JM, Polzin KL, Schmitt RW (1994) Estimates of diapycnal mixing in the abyssal ocean. Science 264:1120–1123
37. Kotz S, Nadarajah S (2000) Extreme value distributions: theory and applications. Imperial College Press, London, p 185